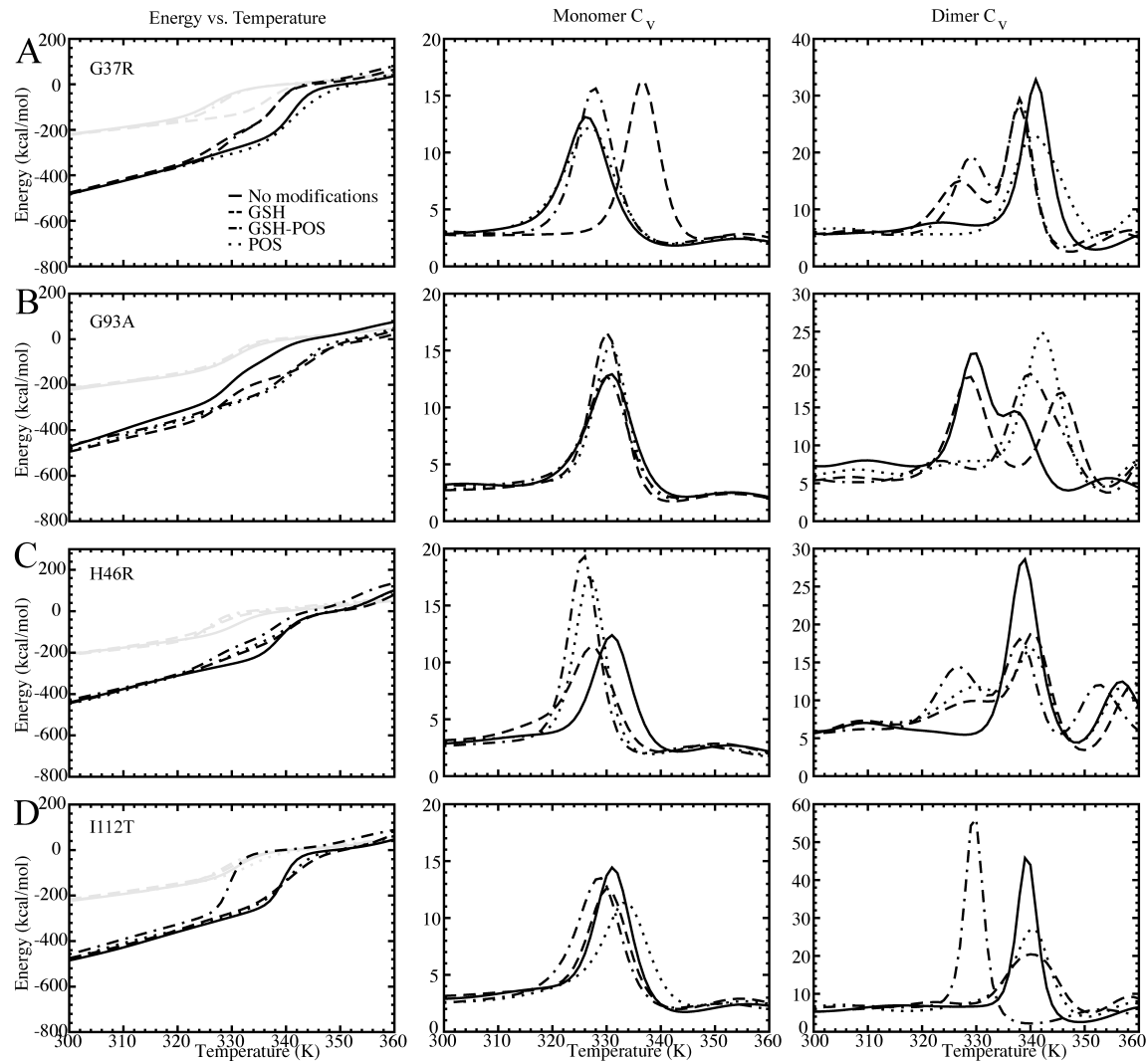


**Structural and Thermodynamic Effects of Post-Translational Modifications in Mutant and Wild Type Cu, Zn Superoxide Dismutase**  
**Elizabeth A. Proctor, Feng Ding, and Nikolay V. Dokholyan**

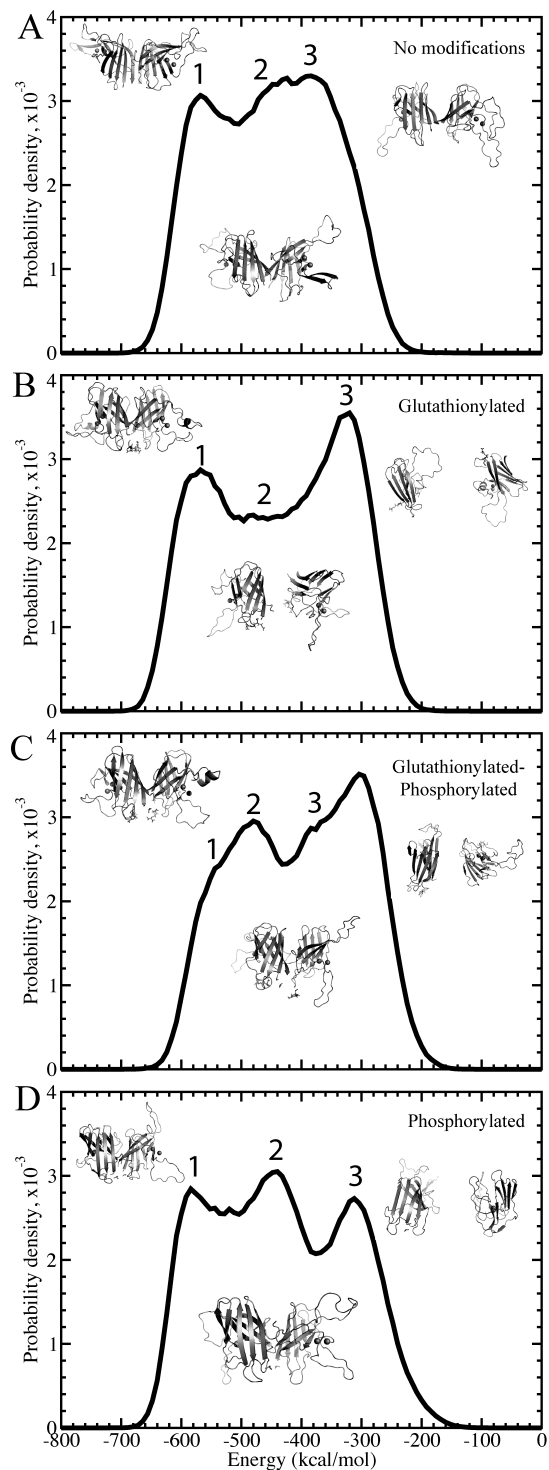
**Supplementary Material:**

**20 Supplementary Figures**  
**4 Supplementary Tables**

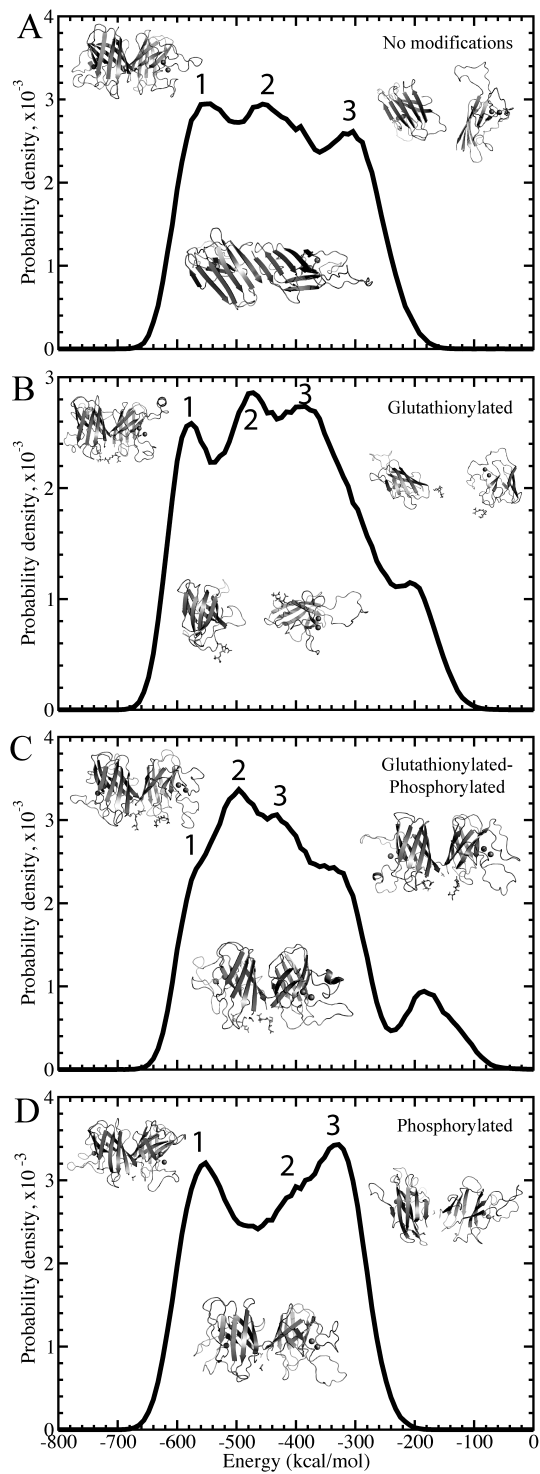
**Supplementary Figure 1. Thermodynamics.** Comparison of (A) G37R, (B) G93A, (C) H46R, and (D) I112T modified and unmodified SOD1. As labeled, the first, second, and third columns, respectively, are: potential energy of the SOD1 complex according to simulation temperature, with monomer curves shown in gray and dimer curves in black; specific heat curves for SOD1 monomer; and specific heat curves for SOD1 dimer. Legend shown for (A) is relevant for all panels.



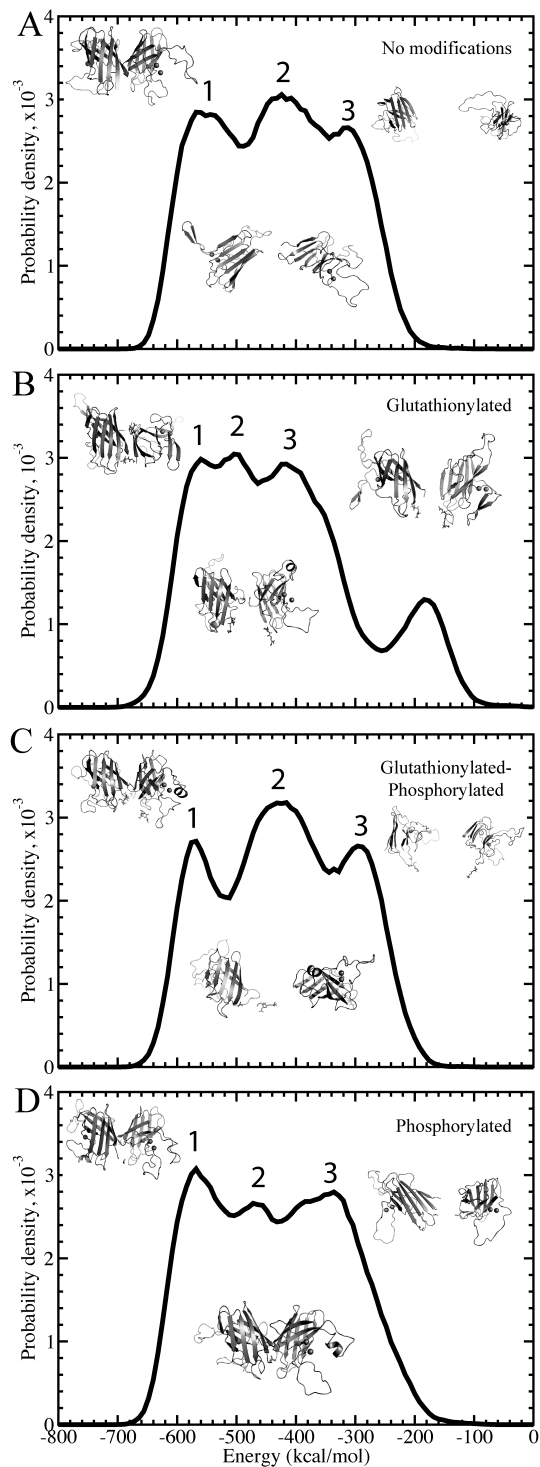
**Supplementary Figure 2. Deciphering the states for A4V.** Distributions of total potential energies are shown with a solid curve. Potential energy is sampled throughout the simulations, at temperatures of 0.55-0.65 kcal/mol•k<sub>B</sub>, for (A) unmodified, (B), glutathionylated, (C) glutathionylated-phosphorylated, and (D) phosphorylated cases of SOD1. The three Gaussian-like curves are highlighted for each species. Representative structures for each of the three states in each species are shown to the right of each plot.



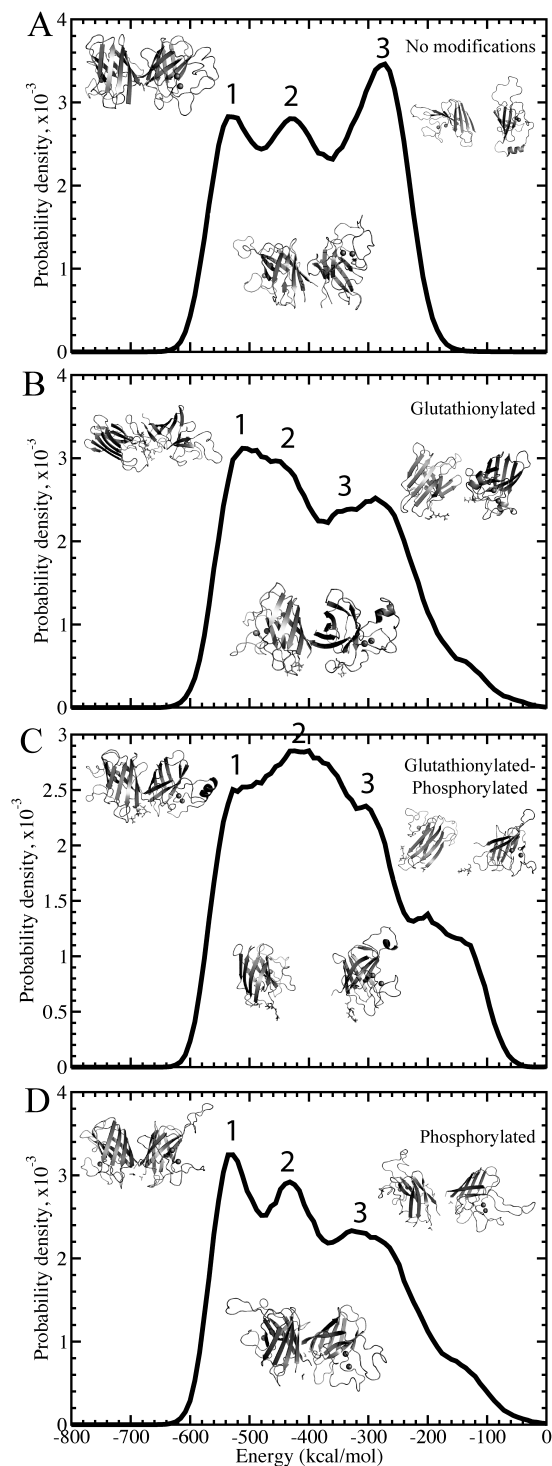
**Supplementary Figure 3. Deciphering the states for G37R.** Distributions of total potential energies are shown with a solid curve. Potential energy is sampled throughout the simulations, at temperatures of 0.5-0.6 kcal/mol•k<sub>B</sub>, for (A) unmodified, (B), glutathionylated, (C) glutathionylated-phosphorylated, and (D) phosphorylated cases of SOD1. The three Gaussian-like curves are highlighted for each species. Representative structures for each of the three states in each species are shown to the right of each plot.



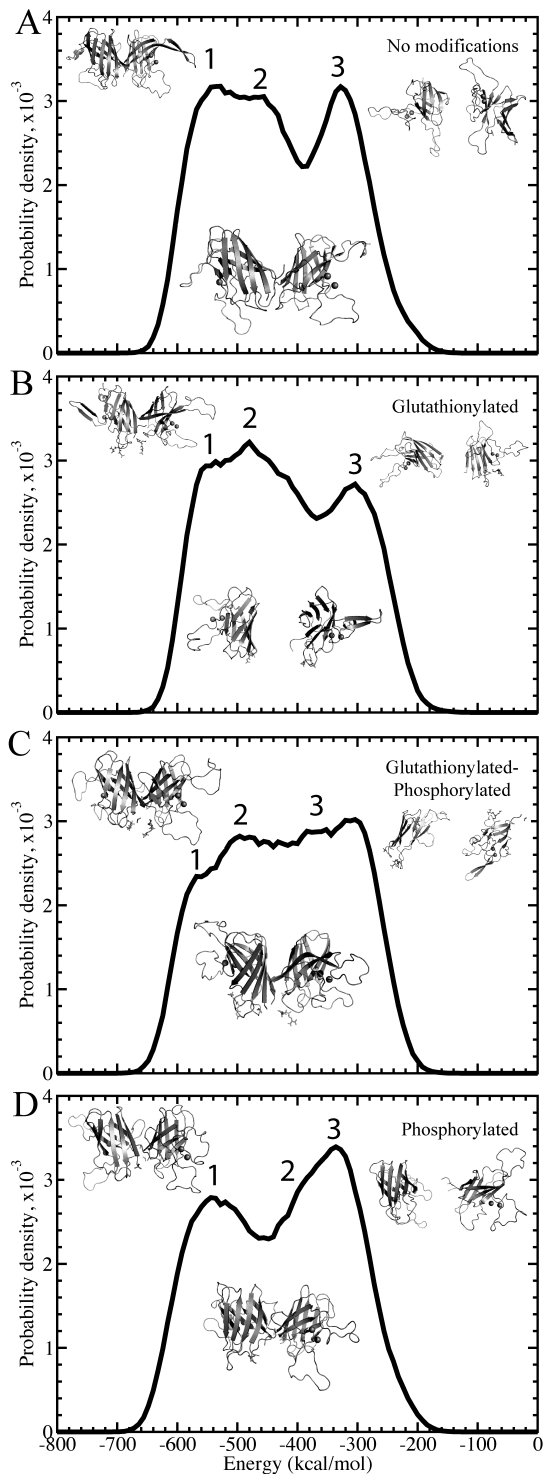
**Supplementary Figure 4. Deciphering the states for G93A.** Distributions of total potential energies are shown with a solid curve. Potential energy is sampled throughout the simulations, at temperatures of 0.5-0.6 kcal/mol•k<sub>B</sub>, for (A) unmodified, (B), glutathionylated, (C) glutathionylated-phosphorylated, and (D) phosphorylated cases of SOD1. The three Gaussian-like curves are highlighted for each species. Representative structures for each of the three states in each species are shown to the right of each plot.



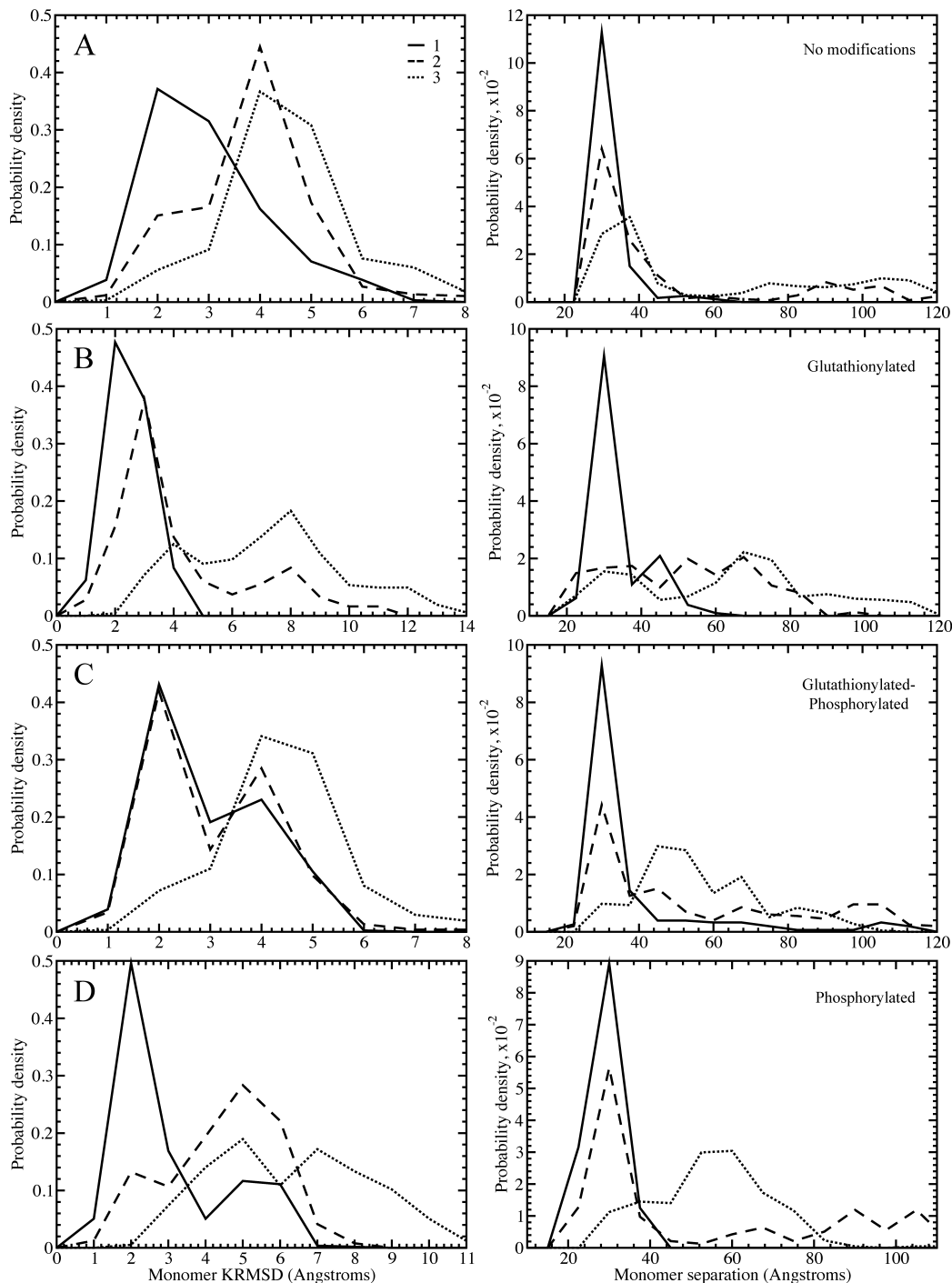
**Supplementary Figure 5. Deciphering the states for H46R.** Distributions of total potential energies are shown with a solid curve. Potential energy is sampled throughout the simulations, at temperatures of 0.5-0.6 kcal/mol•k<sub>B</sub>, for (A) unmodified, (B), glutathionylated, (C) glutathionylated-phosphorylated, and (D) phosphorylated cases of SOD1. The three Gaussian-like curves are highlighted for each species. Representative structures for each of the three states in each species are shown to the right of each plot.



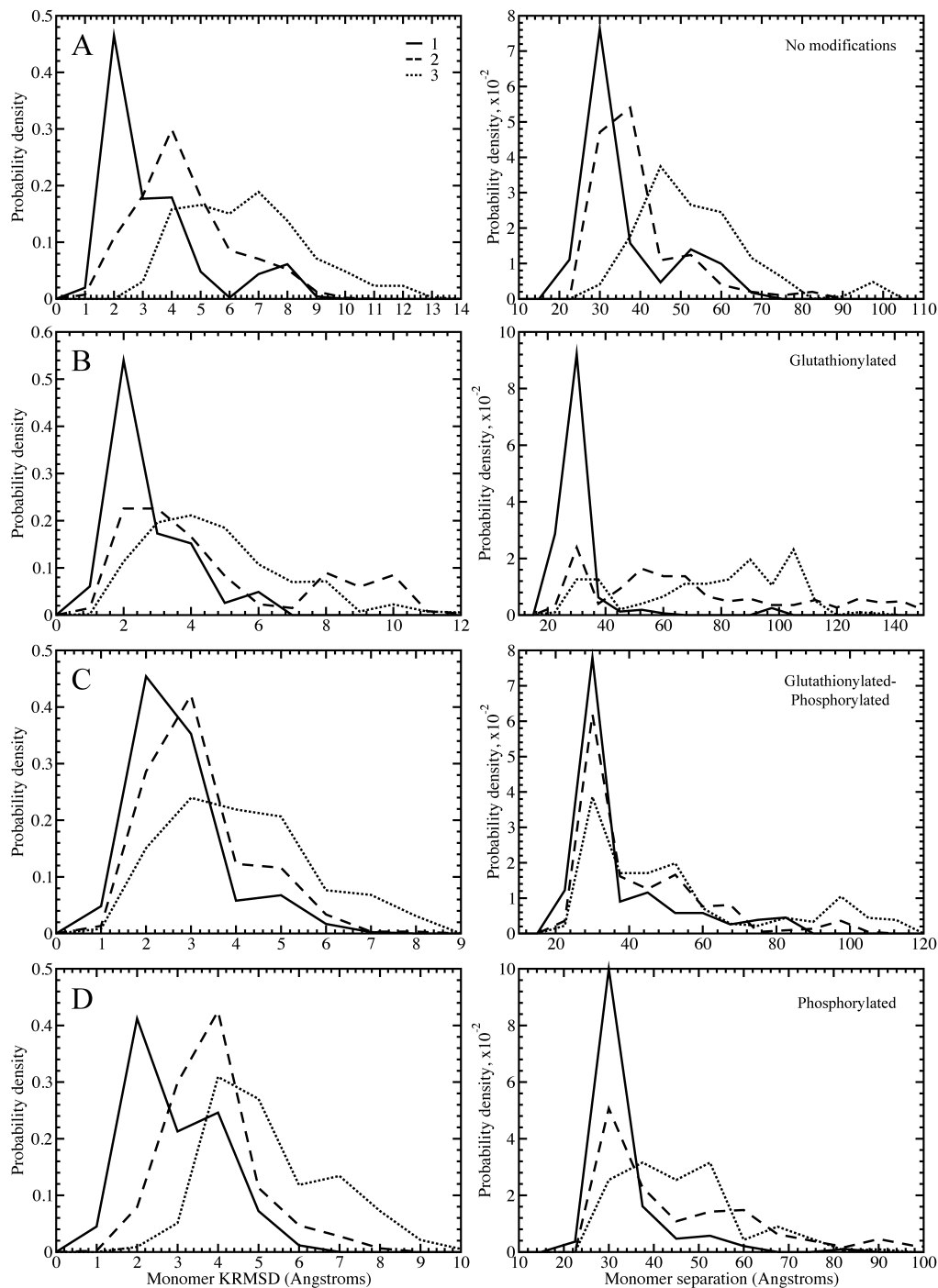
**Supplementary Figure 6. Deciphering the states for I112T.** Distributions of total potential energies are shown with a solid curve. Potential energy is sampled throughout the simulations, at temperatures of 0.5-0.6 kcal/mol•k<sub>B</sub>, for (A) unmodified, (B), glutathionylated, (C) glutathionylated-phosphorylated, and (D) phosphorylated cases of SOD1. The three Gaussian-like curves are highlighted for each species. Representative structures for each of the three states in each species are shown to the right of each plot.



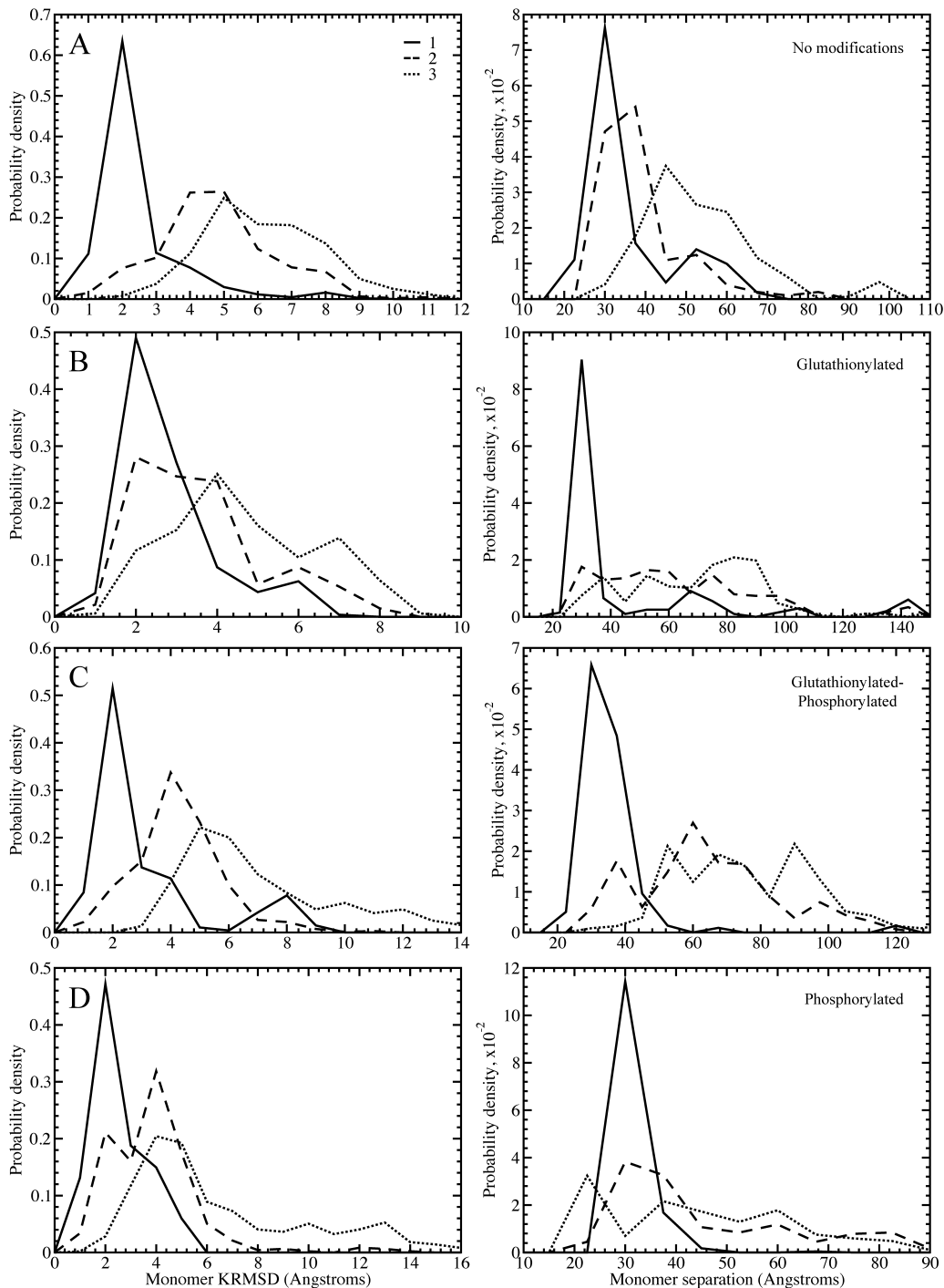
**Supplementary Figure 7. Structural characterization of energetic populations in A4V SOD1.** Distributions of values for the monomer aligned RMSD (Kabsch Root Mean Squared Distance, KRMSD) from the starting structure, used as a measure of  $\beta$ -barrel integrity and unfolding (left column), and the distance between monomer centers of mass, used as a measure of dissociation (right column). We show distributions for (A) unmodified, (B) glutathionylated, (C) glutathionylated-phosphorylated, and (D) phosphorylated A4V SOD1 for the first, second, and third energy populations described in Figure 3. Legend shown for (A) is relevant for all panels.



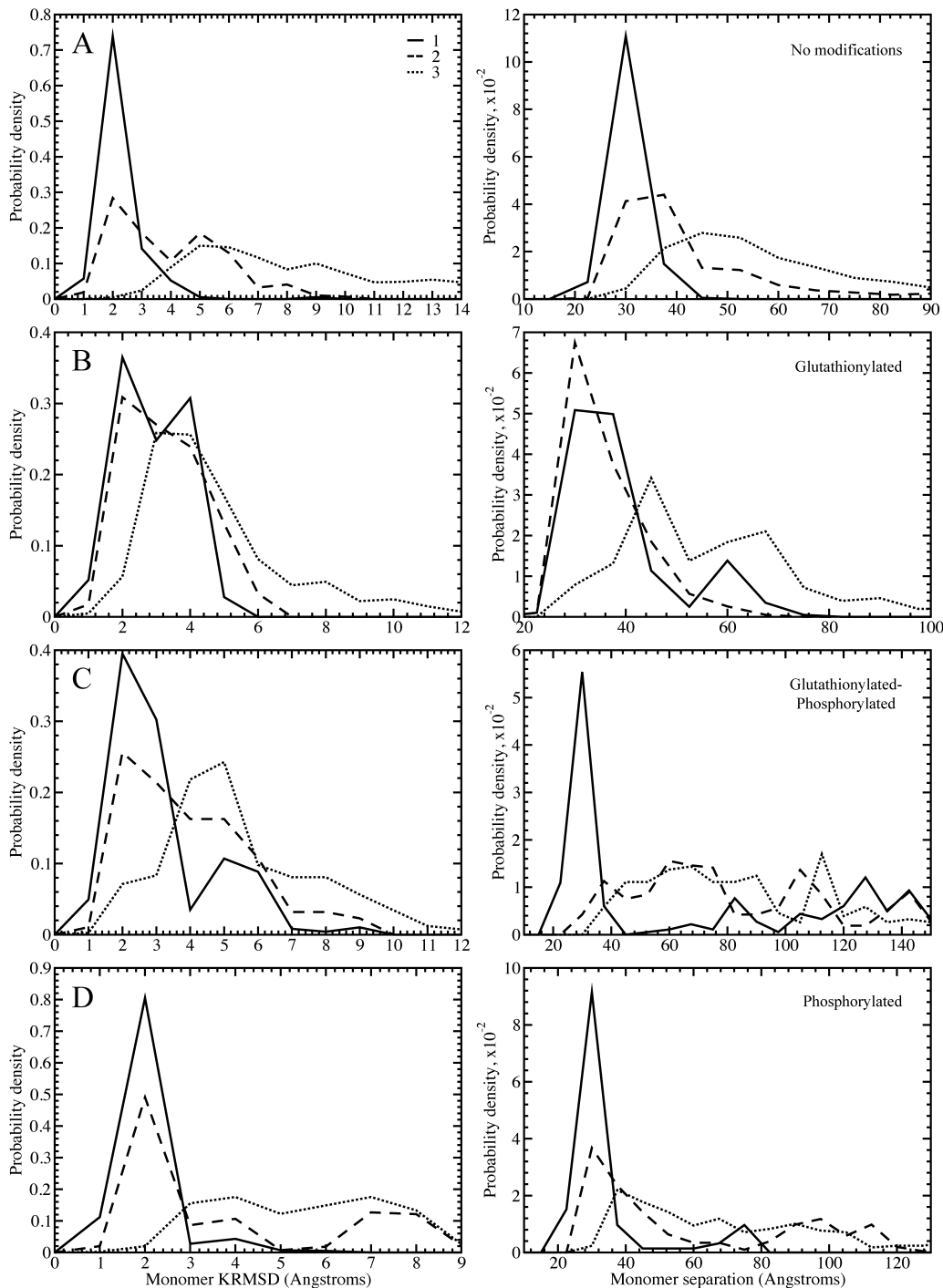
**Supplementary Figure 8. Structural characterization of energetic populations in G37R SOD1.** Distributions of values for the monomer aligned RMSD (Kabsch Root Mean Squared Distance, KRMSD) from the starting structure, used as a measure of  $\beta$ -barrel integrity and unfolding (left column), and the distance between monomer centers of mass, used as a measure of dissociation (right column). We show distributions for (A) unmodified, (B) glutathionylated, (C) glutathionylated-phosphorylated, and (D) phosphorylated G37R SOD1 for the first, second, and third energy populations described in Supplementary Figure 4. Legend shown for (A) is relevant for all panels.



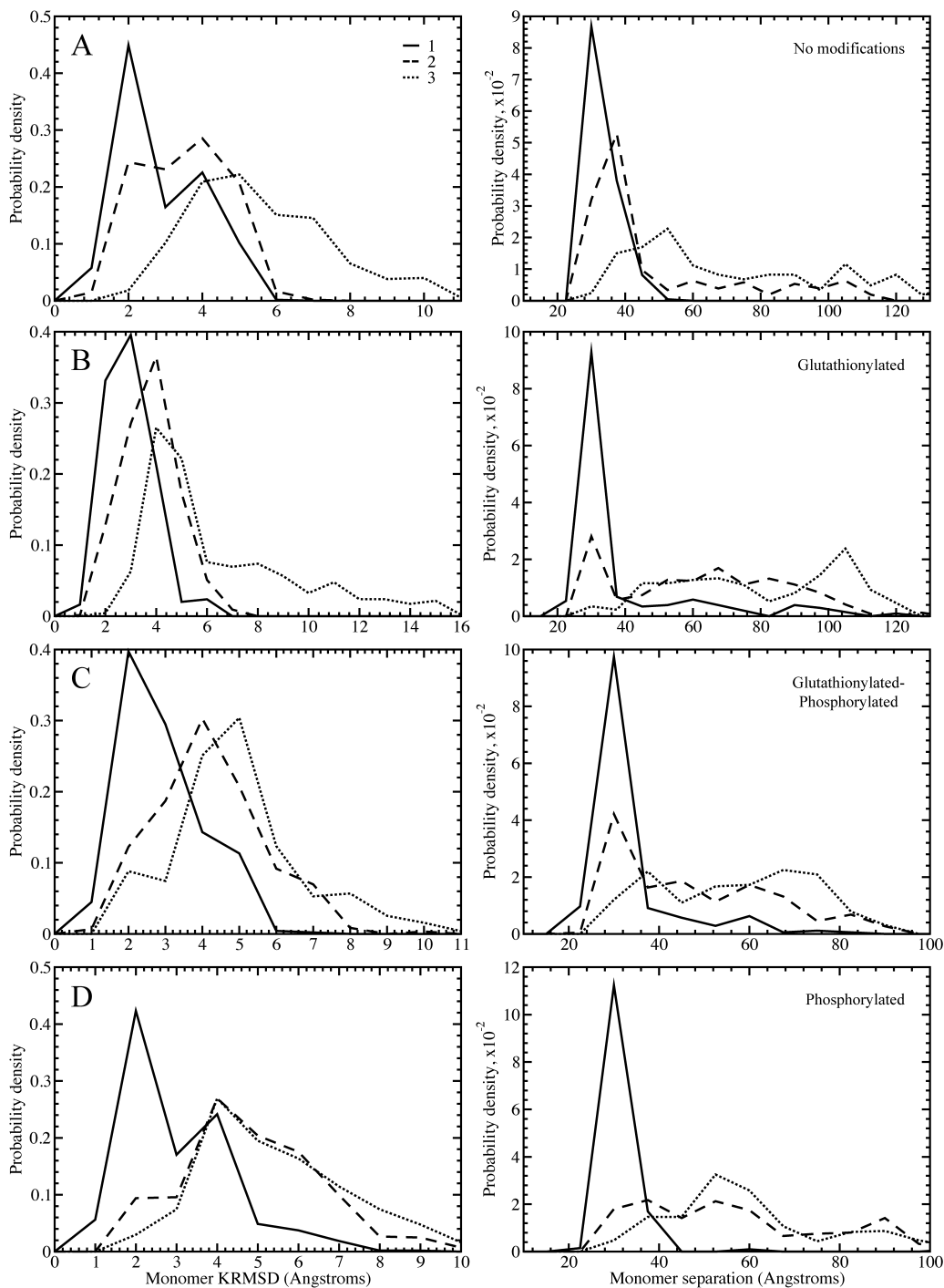
**Supplementary Figure 9. Structural characterization of energetic populations in G93A SOD1.** Distributions of values for the monomer aligned RMSD (Kabsch Root Mean Squared Distance, KRMSD) from the starting structure, used as a measure of  $\beta$ -barrel integrity and unfolding (left column), and the distance between monomer centers of mass, used as a measure of dissociation (right column). We show distributions for (A) unmodified, (B) glutathionylated, (C) glutathionylated-phosphorylated, and (D) phosphorylated G93A SOD1 for the first, second, and third energy populations described in Supplementary Figure 5. Legend shown for (A) is relevant for all panels.



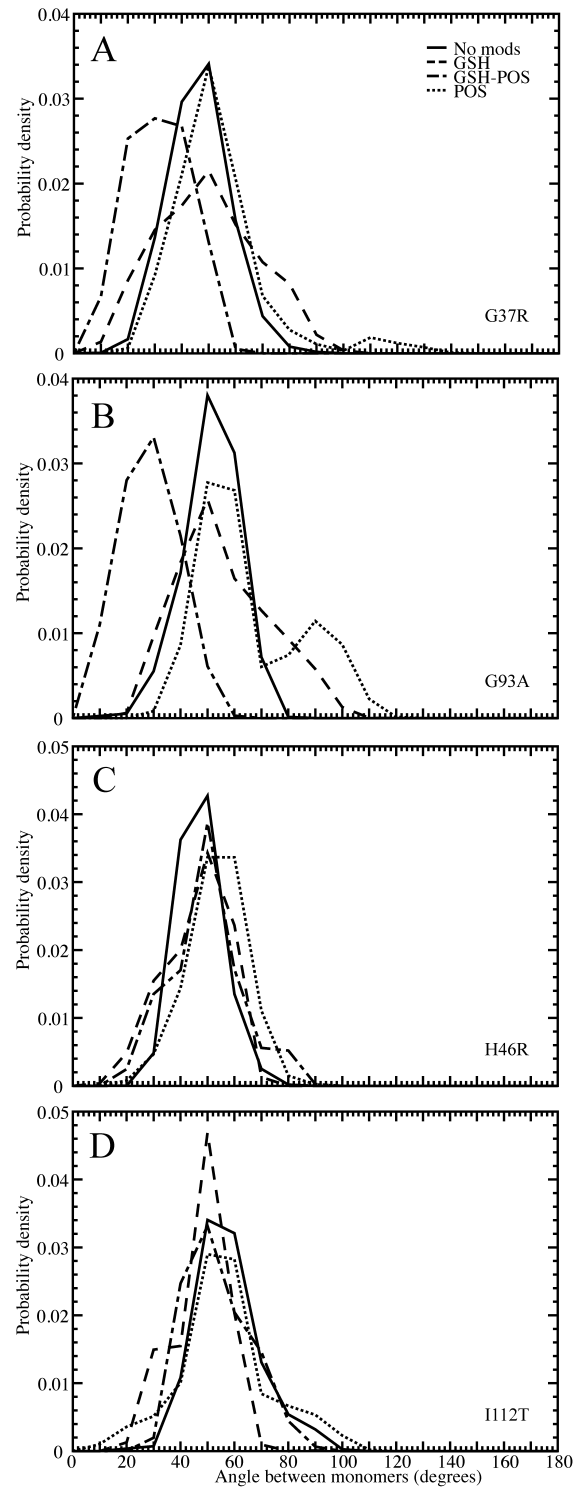
**Supplementary Figure 10. Structural characterization of energetic populations in H46R SOD1.** Distributions of values for the monomer aligned RMSD (Kabsch Root Mean Squared Distance, KRMSD) from the starting structure, used as a measure of  $\beta$ -barrel integrity and unfolding (left column), and the distance between monomer centers of mass, used as a measure of dissociation (right column). We show distributions for (A) unmodified, (B) glutathionylated, (C) glutathionylated-phosphorylated, and (D) phosphorylated H46R SOD1 for the first, second, and third energy populations described in Supplementary Figure 6. Legend shown for (A) is relevant for all panels.



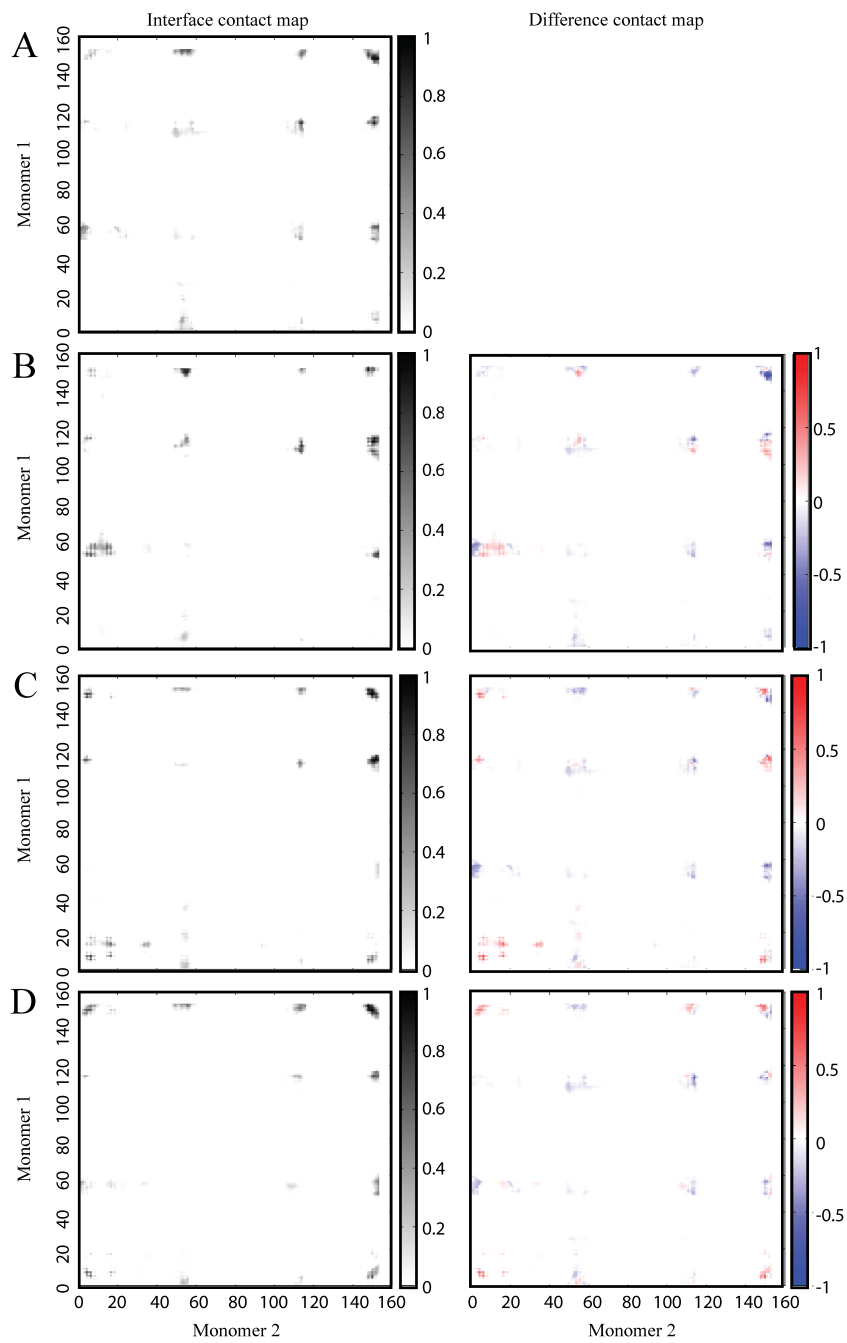
**Supplementary Figure 11. Structural characterization of energetic populations in I112T SOD1.** Distributions of values for the monomer aligned RMSD (Kabsch Root Mean Squared Distance, KRMSD) from the starting structure, used as a measure of  $\beta$ -barrel integrity and unfolding (left column), and the distance between monomer centers of mass, used as a measure of dissociation (right column). We show distributions for (A) unmodified, (B) glutathionylated, (C) glutathionylated-phosphorylated, and (D) phosphorylated I112T SOD1 for the first, second, and third energy populations described in Supplementary Figure 7. Legend shown for (A) is relevant for all panels.



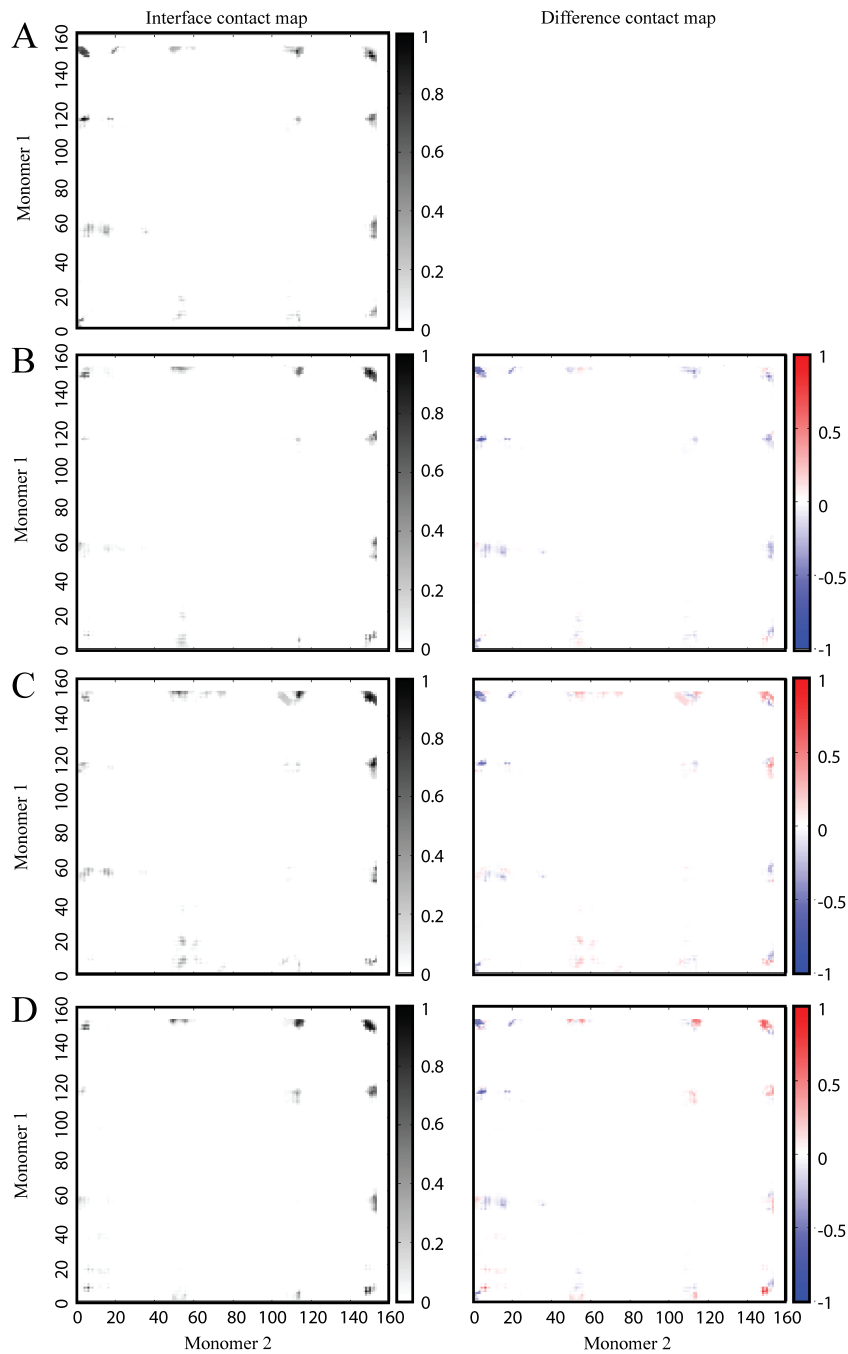
**Supplementary Figure 12. Structural effects of modification on the angle between monomers in the SOD1 dimer.** Depiction of the angle,  $\theta$ , measured between monomers in the SOD1 dimer. Distribution of angle between monomers in equilibrium populations of modified and unmodified (A) G37R, (B) G93A, (C) H46R, and (D) I112T dimer. Legend shown for (A) is relevant for all panels.



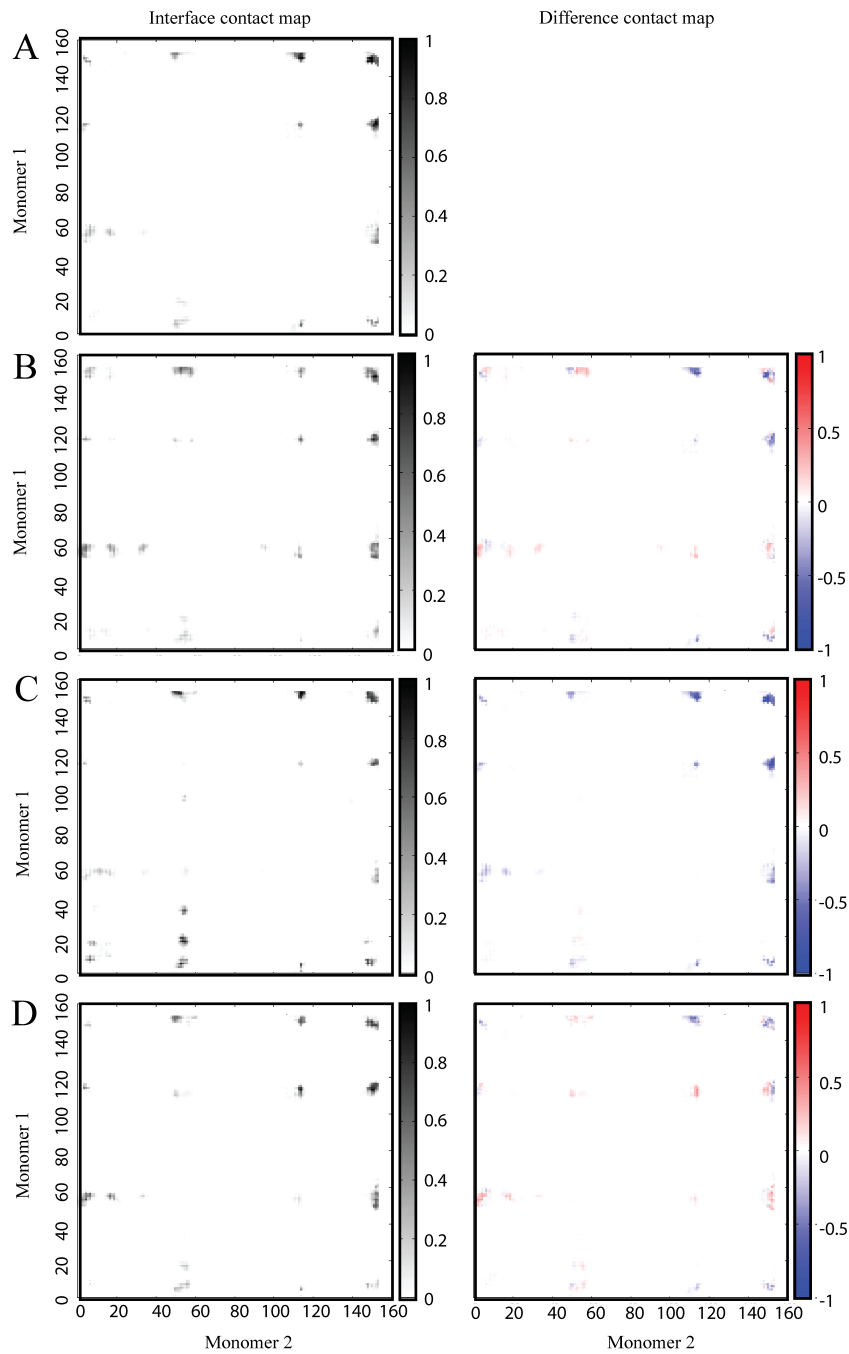
**Supplementary Figure 13. Effects of modifications on the wild-type dimer interface.** Dimer interface contact maps for (A) unmodified, (B) glutathionylated, (C) glutathionylated-phosphorylated, and (D) phosphorylated wild-type SOD1 dimer. Residues for one monomer each are shown on the x- and y-axes. Contact maps in the left column show the frequency of the residue-residue contact, defined as  $C_{\alpha}$ - $C_{\alpha}$  distance of 10 Å or less, over the entire equilibrium simulation. Where applicable, contact maps in the right column show the difference in frequency of the residue-residue contact from the unmodified species.



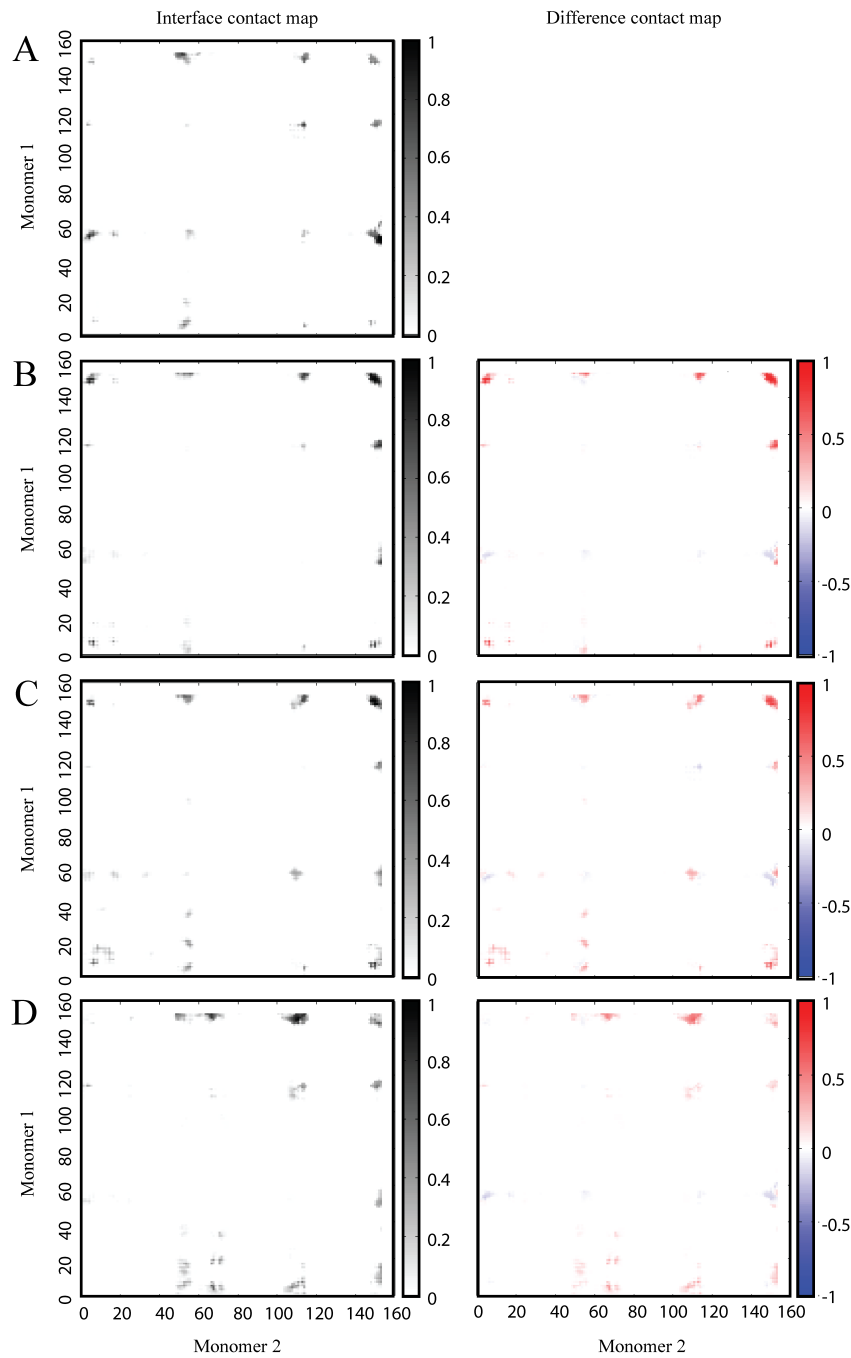
**Supplementary Figure 14. Effects of modifications on the mutant A4V dimer interface.** Dimer interface contact maps for (A) unmodified, (B) glutathionylated, (C) glutathionylated-phosphorylated, and (D) phosphorylated A4V SOD1 dimer. Residues for one monomer each are shown on the x- and y-axes. Contact maps in the left column show the frequency of the residue-residue contact, defined as  $C_{\alpha}$ - $C_{\alpha}$  distance of 10 Å or less, over the entire equilibrium simulation. Where applicable, contact maps in the right column show the difference in frequency of the residue-residue contact from the unmodified species.



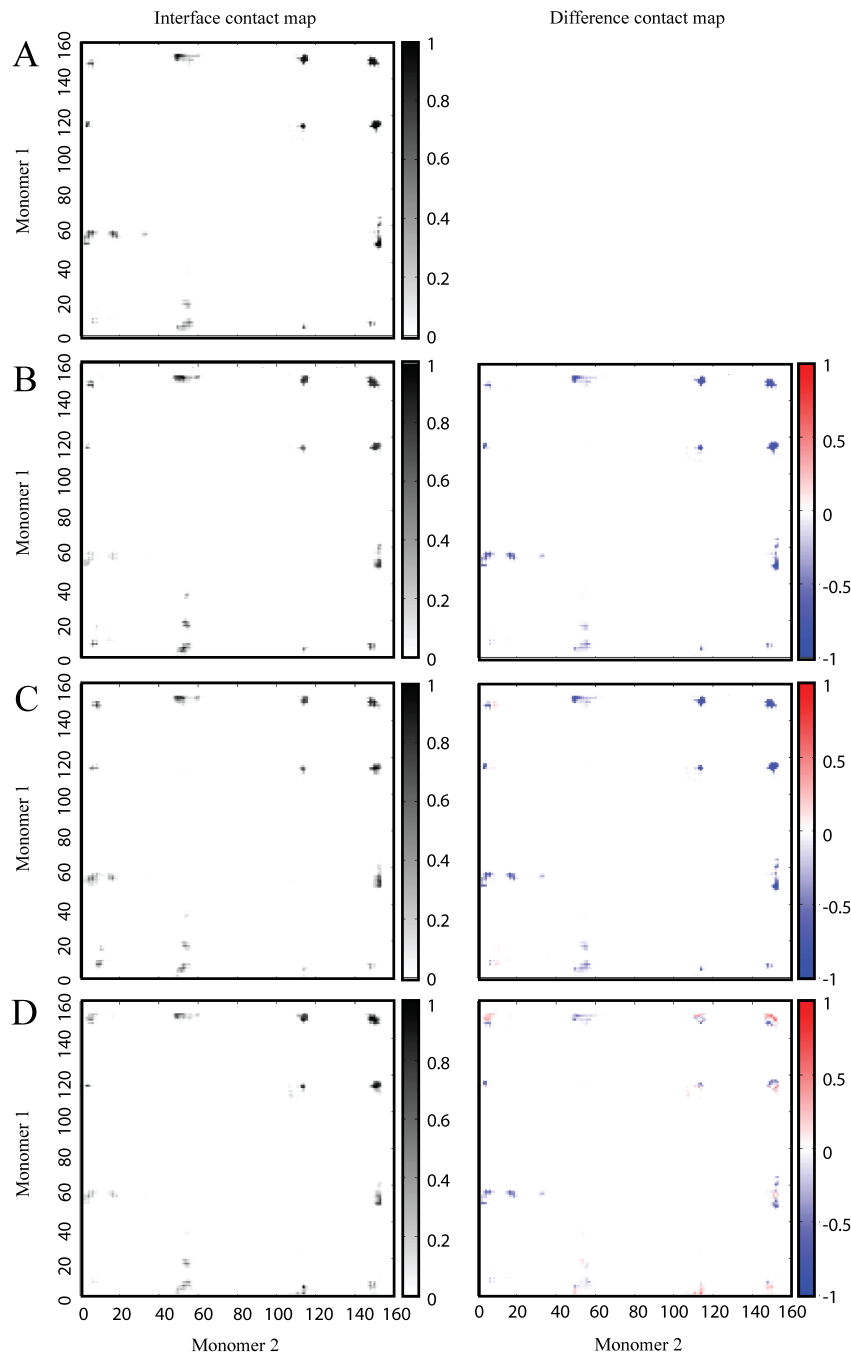
**Supplementary Figure 15. Effects of modifications on the mutant G37R dimer interface.** Dimer interface contact maps for (A) unmodified, (B) glutathionylated, (C) glutathionylated-phosphorylated, and (D) phosphorylated G37R SOD1 dimer. Residues for one monomer each are shown on the x- and y-axes. Contact maps in the left column show the frequency of the residue-residue contact, defined as  $C_{\alpha}$ - $C_{\alpha}$  distance of 10 Å or less, over the entire equilibrium simulation. Where applicable, contact maps in the right column show the difference in frequency of the residue-residue contact from the unmodified species.



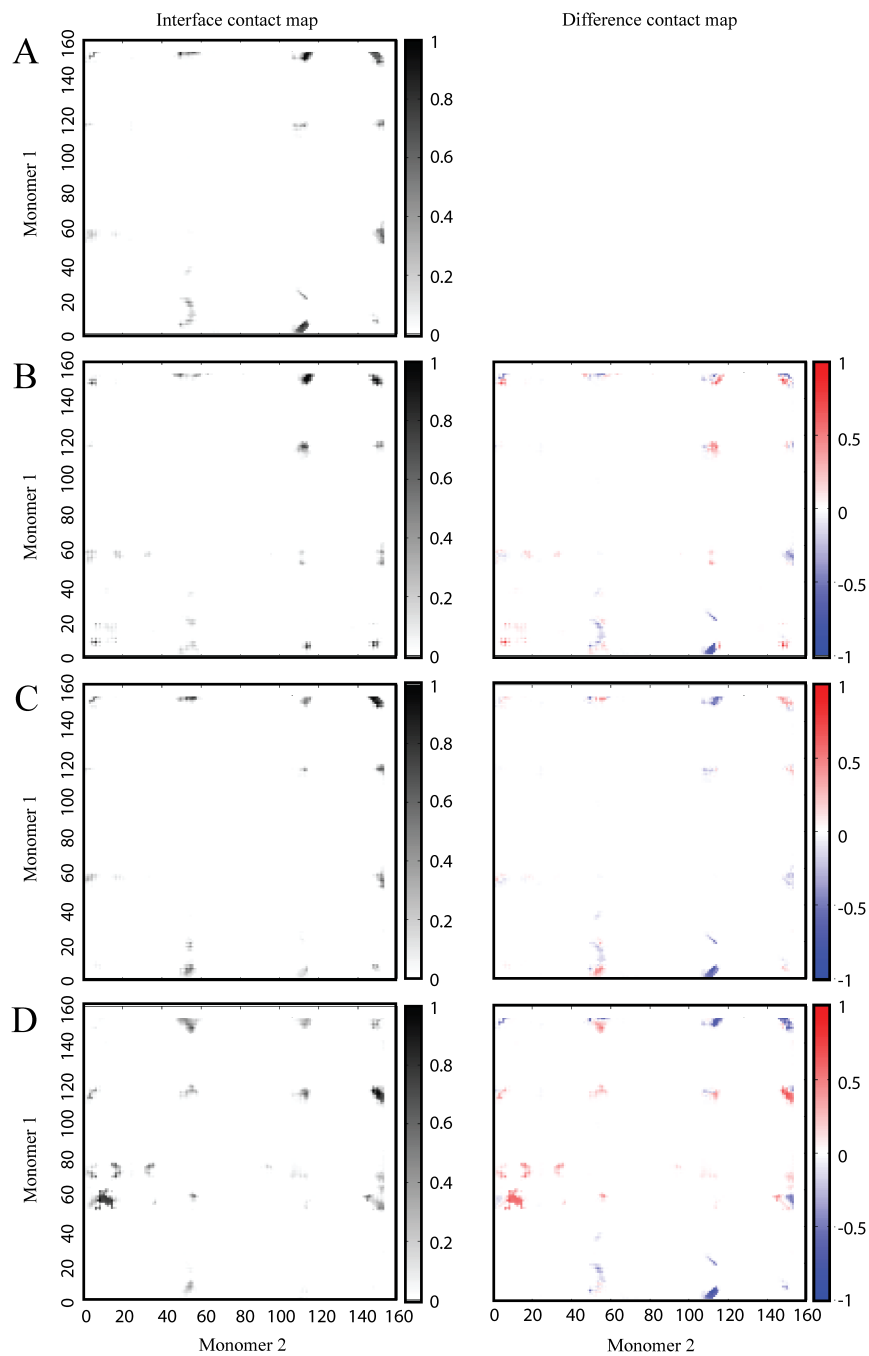
**Supplementary Figure 16. Effects of modifications on the mutant G93A dimer interface.** Dimer interface contact maps for (A) unmodified, (B) glutathionylated, (C) glutathionylated-phosphorylated, and (D) phosphorylated G93A SOD1 dimer. Residues for one monomer each are shown on the x- and y-axes. Contact maps in the left column show the frequency of the residue-residue contact, defined as  $C_{\alpha}$ - $C_{\alpha}$  distance of 10 Å or less, over the entire equilibrium simulation. Where applicable, contact maps in the right column show the difference in frequency of the residue-residue contact from the unmodified species.



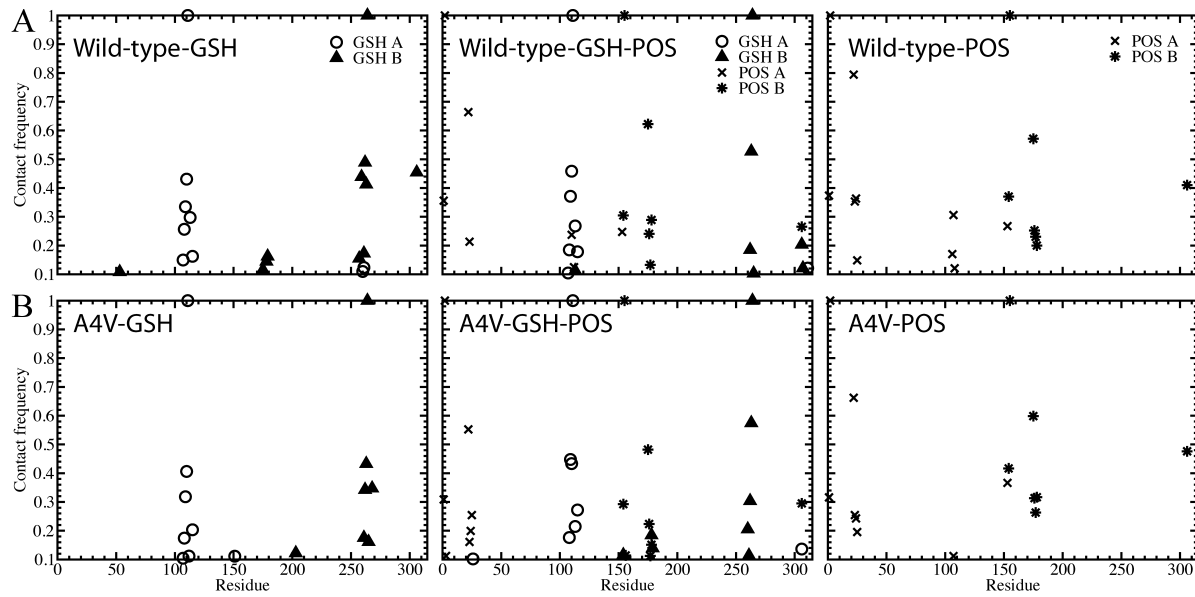
**Supplementary Figure 17. Effects of modifications on the mutant H46R dimer interface.** Dimer interface contact maps for (A) unmodified, (B) glutathionylated, (C) glutathionylated-phosphorylated, and (D) phosphorylated H46R SOD1 dimer. Residues for one monomer each are shown on the x- and y-axes. Contact maps in the left column show the frequency of the residue-residue contact, defined as  $C_{\alpha}-C_{\alpha}$  distance of 10 Å or less, over the entire equilibrium simulation. Where applicable, contact maps in the right column show the difference in frequency of the residue-residue contact from the unmodified species.



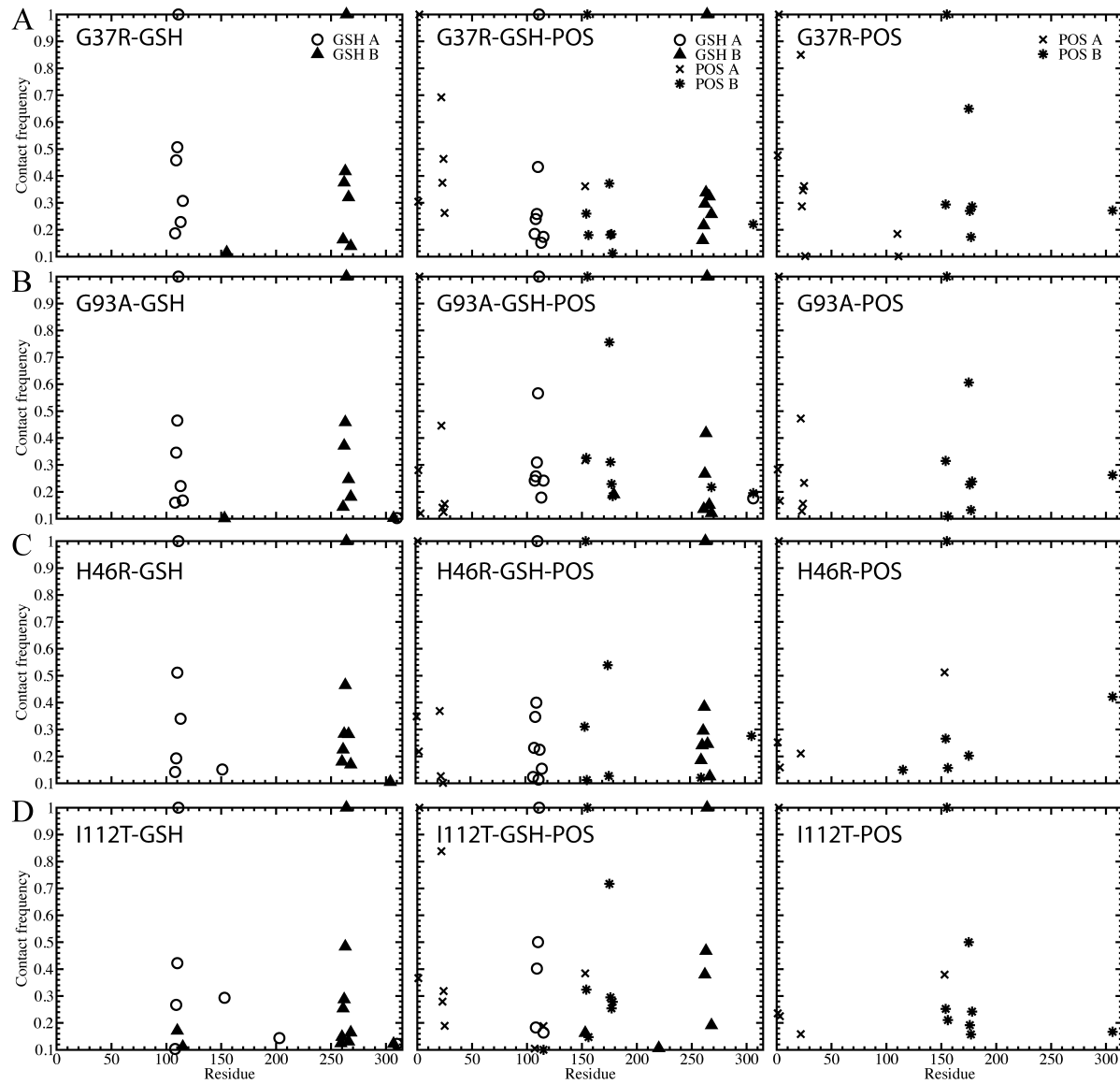
**Supplementary Figure 18. Effects of modifications on the mutant I112T dimer interface.** Dimer interface contact maps for (A) unmodified, (B) glutathionylated, (C) glutathionylated-phosphorylated, and (D) phosphorylated I112T SOD1 dimer. Residues for one monomer each are shown on the x- and y-axes. Contact maps in the left column show the frequency of the residue-residue contact, defined as  $C_{\alpha}-C_{\alpha}$  distance of 10 Å or less, over the entire equilibrium simulation. Where applicable, contact maps in the right column show the difference in frequency of the residue-residue contact from the unmodified species.



**Supplementary Figure 19. Interactions of modification molecules in wild type and A4V.** Interaction frequencies of each modification molecule with each residue of SOD1 for (A) wild-type and (B) A4V. Residues of the second monomer are represented as residues 154-306. Residues 307-314 are in the order: GSH A, POS A, Cu A, Zn A, GSH B, POS B, Cu B, and Zn B, where present, where A and B denote the two monomers. Legends shown for (A) are relevant for all panels.



**Supplementary Figure 20. Interactions of modification molecules in other mutants.** Interaction frequencies of each modification molecule with each residue of SOD1 for (A) G37R, (B) G93A, (C) H46R, and (D) I112T. Residues of the second monomer are represented as residues 154-306. Residues 307-314 are in the order: GSH A, POS A, Cu A, Zn A, GSH B, POS B, Cu B, and Zn B, where present, where A and B denote the two monomers. Legends shown for (A) are relevant for all panels.



**Supplementary Table 1. Dimer transition temperatures.** Major transition temperature of the various dimer species as observed in the energy versus temperature curves and the specific heat plots (Figure 1, Supplementary Figure 1).

		<b>Transition Temperature (K)</b>
Wild-type	<b>No modifications</b>	340
	<b>GSH</b>	339
	<b>GSH-P<sub>i</sub></b>	339
	<b>P<sub>i</sub></b>	343
A4V	<b>No modifications</b>	338
	<b>GSH</b>	331
	<b>GSH-P<sub>i</sub></b>	347
	<b>P<sub>i</sub></b>	339
G37R	<b>No modifications</b>	341
	<b>GSH</b>	338
	<b>GSH-P<sub>i</sub></b>	338
	<b>P<sub>i</sub></b>	340
G93A	<b>No modifications</b>	329
	<b>GSH</b>	329
	<b>GSH-P<sub>i</sub></b>	340
	<b>P<sub>i</sub></b>	342
H46R	<b>No modifications</b>	339
	<b>GSH</b>	341
	<b>GSH-P<sub>i</sub></b>	340
	<b>P<sub>i</sub></b>	339
I112T	<b>No modifications</b>	339
	<b>GSH</b>	340
	<b>GSH-P<sub>i</sub></b>	329
	<b>P<sub>i</sub></b>	340

**Supplementary Table 2. Structural characterization of energetic populations.** Distribution averages for the monomer aligned RMSD from original structure, a measure of  $\beta$ -barrel integrity, and distance between monomer centers of mass, a measure of dissociation. Values shown in each cell are for the first, second, and third energy populations that are described in Figure 2 and Supplementary Figures 2-6. The full distributions of the properties below are shown in Figure 3 and Supplementary Figures 7-11.

		Monomer RMSD (Å)			COM-COM distance (Å)		
		1	2	3	1	2	3
<b>Wild-type</b>	<b>No modifications</b>	1.75	3.40	4.64	33.89	56.46	66.11
	<b>GSH</b>	2.67	3.60	4.26	45.57	65.43	71.84
	<b>GSH-P<sub>i</sub></b>	1.76	3.29	4.16	25.77	41.77	48.08
	<b>P<sub>i</sub></b>	2.07	2.61	5.33	27.51	33.87	49.06
<b>A4V</b>	<b>No modifications</b>	2.47	3.32	4.12	27.55	43.94	57.86
	<b>GSH</b>	1.98	3.75	6.71	29.31	47.37	59.16
	<b>GSH-P<sub>i</sub></b>	2.39	2.52	4.04	33.87	52.14	52.98
	<b>P<sub>i</sub></b>	2.54	3.94	5.89	25.68	49.17	51.66
<b>G37R</b>	<b>No modifications</b>	2.77	3.92	6.05	32.56	34.88	49.444
	<b>GSH</b>	2.19	4.20	4.24	26.67	66.09	72.34
	<b>GSH-P<sub>i</sub></b>	2.16	2.65	3.60	32.64	37.77	48.54
	<b>P<sub>i</sub></b>	2.39	3.36	4.82	28.98	41.93	42.04
<b>G93A</b>	<b>No modifications</b>	1.85	4.28	5.68	31.23	72.26	76.76
	<b>GSH</b>	2.27	3.06	4.16	42.12	58.86	66.71
	<b>GSH-P<sub>i</sub></b>	2.56	3.74	6.56	31.32	60.39	72.91
	<b>P<sub>i</sub></b>	1.97	3.34	6.03	27.94	43.61	43.10
<b>H46R</b>	<b>No modifications</b>	1.61	3.47	7.38	26.29	41.01	51.75
	<b>GSH</b>	2.39	2.73	4.27	34.66	32.35	54.96
	<b>GSH-P<sub>i</sub></b>	2.61	3.44	5.01	65.45	78.02	78.90
	<b>P<sub>i</sub></b>	1.44	3.32	5.17	30.22	55.67	67.25
<b>I112T</b>	<b>No modifications</b>	2.35	2.99	5.09	29.23	45.35	67.88
	<b>GSH</b>	2.44	3.28	5.99	34.57	58.86	76.44
	<b>GSH-P<sub>i</sub></b>	2.37	3.68	4.47	29.30	44.16	53.21
	<b>P<sub>i</sub></b>	2.50	4.35	4.97	27.57	52.69	56.29

**Supplementary Table 3. Energetic populations.** Peak values of the energetic populations observed in Figure 2 and Supplementary Figures 2-6, and the resulting energy differences between the states.

		Peak energy of population (kcal/mol)			Energy difference between states (kcal/mol)		
		1	2	3	$\Delta E_{1 \rightarrow 2}$	$\Delta E_{2 \rightarrow 3}$	$\Delta E_{1 \rightarrow 3}$
<b>Wild-type</b>	<b>No modifications</b>	-567	-433	-340	134	93	227
	<b>GSH</b>	-562	-497	-414	65	83	148
	<b>GSH-P<sub>i</sub></b>	-563	-412	-335	151	77	228
	<b>P<sub>i</sub></b>	-549	-459	-331	90	128	218
<b>A4V</b>	<b>No modifications</b>	-566	-439	-382	127	57	184
	<b>GSH</b>	-569	-449	-321	120	128	248
	<b>GSH-P<sub>i</sub></b>	-553	-477	-368	76	109	185
	<b>P<sub>i</sub></b>	-580	-443	-308	137	135	272
<b>G37R</b>	<b>No modifications</b>	-553	-449	-304	104	145	249
	<b>GSH</b>	-576	-474	-387	102	87	189
	<b>GSH-P<sub>i</sub></b>	-562	-497	-428	65	69	134
	<b>P<sub>i</sub></b>	-552	-411	-332	141	79	220
<b>G93A</b>	<b>No modifications</b>	-556	-419	-309	137	110	247
	<b>GSH</b>	-559	-496	-420	63	76	139
	<b>GSH-P<sub>i</sub></b>	-569	-426	-292	143	134	277
	<b>P<sub>i</sub></b>	-568	-468	-340	100	128	228
<b>H46R</b>	<b>No modifications</b>	-530	-426	-279	104	147	251
	<b>GSH</b>	-512	-448	-339	64	109	173
	<b>GSH-P<sub>i</sub></b>	-508	-407	-301	101	106	207
	<b>P<sub>i</sub></b>	-530	-435	-311	95	124	219
<b>I112T</b>	<b>No modifications</b>	-539	-461	-325	78	136	214
	<b>GSH</b>	-545	-473	-306	72	167	239
	<b>GSH-P<sub>i</sub></b>	-561	-491	-371	70	120	190
	<b>P<sub>i</sub></b>	-535	-400	-335	135	65	200

**Supplementary Table 4. Torsional angle between SOD1 monomers.** Peak values of the distributions of the angle between monomers observed in Figure 4 and Supplementary Figure 12.

		Angle between monomers (°)
Wild-type	No modifications	60
	GSH	40
	GSH-P <sub>i</sub>	40
	P <sub>i</sub>	71
A4V	No modifications	45
	GSH	50
	GSH-P <sub>i</sub>	40
	P <sub>i</sub>	60
G37R	No modifications	46
	GSH	50
	GSH-P <sub>i</sub>	30
	P <sub>i</sub>	50
G93A	No modifications	53
	GSH	51
	GSH-P <sub>i</sub>	29
	P <sub>i</sub>	55
H46R	No modifications	47
	GSH	50
	GSH-P <sub>i</sub>	50
	P <sub>i</sub>	55
I112T	No modifications	55
	GSH	50
	GSH-P <sub>i</sub>	50
	P <sub>i</sub>	55